



Contents lists available at ScienceDirect

Journal of King Saud University – Science

journal homepage: www.sciencedirect.com

Original article

de novo pyrimidine synthesis pathway inhibition reduces motility virulence of *Pseudomonas aeruginosa* despite complementation

Abdurahman A. Niazy^{a,b,*}, Rhodanne Nicole A. Lambarte^b, Hamdan S. Alghamdi^c^a Department of Oral Medicine and Diagnostic Sciences, College of Dentistry, King Saud University, Riyadh, Saudi Arabia^b Molecular and Cell Biology Laboratory, Prince Naif bin AbdulAziz Health Research Center, King Saud University, Riyadh, Saudi Arabia^c Department of Periodontics and Community Dentistry, College of Dentistry, King Saud University, Riyadh, Saudi Arabia

ARTICLE INFO

Article history:

Received 28 January 2021

Revised 17 March 2022

Accepted 14 April 2022

Available online 22 April 2022

Keywords:

Pseudomonas aeruginosa

pyrimidine synthesis pathway

motility

virulence factors

biofilm formation

pyrE

mutation

ABSTRACT

Objectives: Finding alternative methods to overcome antibiotic resistance in the medically important bacterium *Pseudomonas aeruginosa* has become increasingly vital as antibiotic resistance becomes more difficult to overcome. DNA synthesis inhibition is a strategy that has been used to inhibit cancer cells from proliferating by using pyrimidine analogues. Gateway site-directed mutagenesis is an effective way to create precise knockouts which creates good models to understand the relationship between biochemical pathways and the physiology of the organism. This article demonstrates the effect of pyrimidine synthesis inhibition on the motility virulence and physiology of *P. aeruginosa*.

Methods: Wild type *Pseudomonas aeruginosa* (PA01) was genetically modified using gateway cloning technology to inhibit the pyrimidine synthesis pathway through the complete knockout of the *pyrE* gene. The mutant strain was compared to the wild type PA01 in terms of its twitching, swarming and swimming motility forms and biofilm formation abilities. In addition to that, the production of the bacterial surfactant, rhamnolipids, was also measured.

Results and conclusions: The inhibition of the pyrimidine synthesis pathway resulted in significant reduction in motility and biofilm capabilities, despite complementing the mutation with uracil to bypass the mutation. Inhibition of the pyrimidine synthesis pathway is thus an effective way to reduce the virulence of *Pseudomonas aeruginosa*. Even though the bacterium is able to acquire pyrimidines from its surrounding, it was not sufficient enough to overcome the effects of the mutation.

© 2022 The Authors. Published by Elsevier B.V. on behalf of King Saud University. This is an open access article under the CC BY license (<http://creativecommons.org/licenses/by/4.0/>).

Abbreviations: $\Delta pyrE$, *pyrE* mutant; $\Delta pyrE+U$, $\Delta pyrE$ supplemented with uracil; 5-FU, fluorouracil; CTAB, cetyltrimethylammonium bromide; CF, cystic fibrosis; CTP, cytosine triphosphate; DHODase, dihydroorotate dehydrogenase; LB, Luria broth; OMP, orotate monophosphate; PA01, *Pseudomonas aeruginosa* wild type; PMNs, polymorphonuclear neutrophils; PRPP, phosphoribosyl pyrophosphate; TS, thymidylate synthase; UMP, uracil monophosphate; UTP, uracil triphosphate; WT, wild type.

* Corresponding author at: Department of Oral Medicine and Diagnostic Sciences, College of Dentistry, King Saud University, Riyadh, Saudi Arabia.

E-mail addresses: aaniazzy@ksu.edu.sa (A.A. Niazy), rlambarte@ksu.edu.sa (R.N.A. Lambarte), dalghamdi@ksu.edu.sa (H.S. Alghamdi).

Peer review under responsibility of King Saud University.

1. Introduction

Pseudomonas aeruginosa (*P. aeruginosa*), a Gram-negative opportunistic bacterium, can cause acute and chronic infections in patients with suppressed immune systems, undergoing cancer chemotherapy, and with cystic fibrosis (Horcajada et al., 2019; Zifodya and Crothers, 2019). *P. aeruginosa* is an important cause of mortality in patients suffering from cystic fibrosis (CF), a devastating genetic disease commonly prevalent among Caucasians (Parkins et al., 2018). Although characterized by chronic lung disease, electrolyte abnormalities and pancreatic insufficiency; the high associated mortality rates of CF is primarily attributed to the formation of mucoid-alginate and biofilms by *P. aeruginosa* (Malhotra et al., 2019). Its pathogenicity is dictated by a variety of virulence factors including synthesis of extracellular toxins, proteases, hemolysins and exopolysaccharides (Jurado-Martín et al., 2021); in addition to its motility and biofilm production capacity (Bains et al., 2012; Kazmierczak et al., 2015; Redfern et al.,



Production and hosting by Elsevier

<https://doi.org/10.1016/j.jksus.2022.102040>

1018-3647/© 2022 The Authors. Published by Elsevier B.V. on behalf of King Saud University.

This is an open access article under the CC BY license (<http://creativecommons.org/licenses/by/4.0/>).

2021). The three major methods by which *P. aeruginosa* exhibits motility are swimming, twitching, and swarming (Burrows, 2012). While the polar flagellum aids in its swimming-type motility through liquid and extremely soft media, type IV pilus enables twitching (Kazmierczak et al., 2015). On the contrary, swarming on semi-solid surfaces is achieved through utilization of both type IV pili and flagella (Kühn et al., 2021; Talà et al., 2019). The motility of *P. aeruginosa* combined with its ability to produce proteins and polysaccharides, enables it to attach to and colonize surfaces forming biofilms, which are considered a key factor in its pathogenicity (Kazmierczak et al., 2015).

The alginate exopolysaccharide exclusively synthesized by *P. aeruginosa*, in addition to enhancing the ability of the organism to propel and colonize lung surfaces, helps it to establish a quorum sensing microbial environment, which evades host defenses and antimicrobial therapy (Chadha et al., 2021; Niazy, 2021). Novel therapies suggested for the treatment of CF include mechanisms of inhibiting biofilm formation and alginate synthesis by *P. aeruginosa* through the use of non-toxic drugs, regulatory proteins, and altering bio-synthetic pathways (Behzadi et al., 2021; Srinivasan et al., 2021). One reportedly achievable strategy is by means of regulating pyrimidine biosynthesis in microorganisms, which conventionally progresses through the *de novo* or salvage pathway (O'Donovan and Neuhard, 1970; Ralli et al., 2007).

The *de novo* pyrimidine synthesis pathway has been studied thoroughly in *P. aeruginosa* (Beckwith et al., 1962; O'Donovan and Neuhard, 1970; O'toole and Kolter, 1998) and has shown to be an important aspect in its production of virulence factors (Hosseinidoust et al., 2013). Moreover, mutations at different sites within this pathway could lead to different outcomes in terms of virulence factor production by *P. aeruginosa* (Niazy and Hughes, 2015; Ralli et al., 2007). Pyrimidine regulation could be achieved either at the enzymatic or transcriptional level, with the former being a feedback mechanism wherein increased cytosine triphosphate (CTP) and uracil triphosphate (UTP) lead to the decrease of pyrimidine enzyme activities and the latter targeting genes involved in the pathway (Niazy and Hughes, 2015). The first three steps in the pyrimidine pathway involves genes namely *pyrB* encoding aspartate transcarbamylase, *pyrC* encoding dihydroorotase, and *pyrD* encoding dihydroorotate dehydrogenase, which together catalyzes the production of orotate from carbamoyl phosphate and aspartate (Womack and O'Donovan, 1978). Secondly, the orotate phosphoribosyltransferase catalysis, a crucial step of the pathway, encoded by the *pyrE* gene resulting to the orotate monophosphate (OMP) synthesis from orotate and phosphoribosyl pyrophosphate (PRPP). This reaction is followed by the final step in the *de novo* pyrimidine pathway, wherein OMP decarboxylase encoded by *pyrF* results in decarboxylation of OMP to form uracil monophosphate (UMP) (Womack and O'Donovan, 1978). While mutations in *pyrE* and *pyrF* could lead to secretion and accumulation of orotate in bacteria (Womack and O'Donovan, 1978), a sim-

ilar phenotype was also reported in humans exhibiting orotic aciduria (Winkler and Suttle, 1988).

Even though previous studies have reported a decrease in virulence factors as a result of orotate accumulation following mutation in *pyrE* (Garavaglia et al., 2012; Niazy and Hughes, 2015; Womack and O'Donovan, 1978;), the specific mutant phenotype in *P. aeruginosa* has not been exhaustively evaluated since. Therefore, this study aimed to determine the effect of disrupting the *de novo* pyrimidine synthesis pathway at *pyrE* on the pathogenicity of *P. aeruginosa*, in terms of motility and biofilm formation.

2. Materials and methods

2.1. Construction of mutant

2.1.1. Synthesis of mutant *pyrE* fragment

The *pyrE* mutant ($\Delta pyrE$) was constructed utilizing Gateway[®] cloning technology (Invitrogen, CA, USA) according to the protocol previously described (Choi and Schweizer, 2005) and has been detailed in our previous work (Niazy and Hughes, 2015). Wild type (WT) *P. aeruginosa* strain PA01 (prototroph; Brichta et al., 2004) was used in all experimental analyses (Table 1). Briefly, the 74 bps fragment from *pyrE* (642 bps) was replaced by the *aacC1* gentamicin-resistant gene. PCR amplification of the modified *pyrE* was configured to: 95 °C for 2 min, 95 °C for 30 s, 50 °C for 30 s, 68 °C for 90 s for 30 cycles and 68 °C for 7 min using the Q5[®] High Fidelity 2X Master Mix (New England Biolabs (NEB), Ipswich, MA). After PCR amplification and addition of *attB* overhangs on the 5' end, running in tandem was the amplification of the gentamicin-resistant gene from the pPS856 plasmid. Using primers that had overhangs that were complementary to the *aacC1* gene in addition to the *attB* overhangs, a PCR was done to attach all three fragments together resulting in a mutant form of *pyrE*-GM with an insertion of a gentamicin-resistant gene replacing bases 337 to 411 with the following conditions: 95 °C for 2 min, 95 °C for 30 s, 50 °C for 30 s, 68 °C for 90 s for 30 cycles and finally 68 °C for 7 min using the Phusion[®] Hot Start Flex DNA Polymerase kit (NEB, MA, USA) (Niazy and Hughes, 2015). All amplicons were analyzed by agarose electrophoresis and corresponding bands were cut out of the gel and purified using PureLink[®] Quick Gel Extraction Kit (Invitrogen, MA, USA) (Table 2).

2.1.2. Construction of donor and gateway plasmids

The connected fragment was then mixed with the enzyme Gateway[®] BP clonase[®] and pDONR221 plasmid from Invitrogen (Carlsbad, CA, USA) utilizing manufacturer's instructions. After recombination, the recombinant plasmid was transformed into *E. coli* (DH5 α) and plated on Luria Broth (LB) agar plates containing 60 μ g/ml kanamycin. The kanamycin-resistant colonies were selected for plasmid extraction using the Invitrogen

Table 1

Bacterial strains, plasmids, genotypes, and source of plasmids used in this study to construct the *pyrE* mutation using Gateway[®] cloning.

Strain or plasmid	Genotype of strain or plasmid	Source/Reference
<i>P. aeruginosa</i> PA01 PA0pyrE ⁻	Prototroph PA01 <i>pyrE</i> Δ	Brichta et al., 2004
<i>E. coli</i> DH5 α	<i>recA1 hsdR17 endA1 supE44 thi-1 relA1 gyrA96</i> Δ (<i>argF-lacZYA</i>)U169 ϕ 80 <i>lacZ</i> Δ M15	Bethesda Research Laboratories, 1986
pDONR221	<i>Kan^R</i> , <i>ccdB</i> suicide gene, <i>attP</i> cloning sites	Invitrogen
pEX18ApGW	<i>AP^R</i> (<i>Cb^R</i>), <i>sacB^R</i> , gateway vector, <i>attR</i> cloning sites, <i>ccdB</i> suicide gene	Dr. H. Schweizer
pDONRpyrEGM	<i>GM^R</i> , <i>pyrE</i> -GM 1700 bp insert donor plasmid	This study
pEX18pyrEGM	<i>GM^R</i> , <i>pyr</i> -GM 1700 bp insert gateway plasmid	This study
pUCP20	<i>AP^R</i> (<i>Cb^R</i>) PA01 replicative control plasmid	Dr. H. Schweizer
pPS856	<i>GM^R</i> for extraction of <i>GM^R</i> gene	Dr. H. Schweizer

Table 2List of primers, their sequences and amplification targets to construct the *pyrE* mutation using Gateway® cloning.

Primer name	Sequence	Amplification target
pyrEUSF	TACAAAAAAGCAGGCTATGCAGGCGTATCA	Forward primer of the upstream region of <i>pyrE</i>
pyrEUSR	TCAGAGCGCTTTTGAAGCTAATTCGCGTGGTCCTTGGCTTCTTGGGTTGAAGCA	Reverse primers of the upstream region of <i>pyrE</i>
pyrEDSF	AGGAAGCTCAAGATCCCAATTCGGCAGATCATCGACGCCAGGGCGCCA	Forward primers of the downstream region of <i>pyrE</i>
pyrEDSR	TACAAGAAAGCTGGGTTTCAGATACCGTATT	Reverse primer of the downstream region of <i>pyrE</i>
Gm-F	CGAATTAGCTTCAAAGCGCTCTGA	Forward primer for <i>aacC1</i> gentamicin resistance cassette from pPS856
Gm-F	CGAATTGGGGATCTTGAAGTTCT	Reverse primer for <i>aacC1</i> gentamicin cassette from pPS856
GW-attB1	GGGGACAAGTTGTACAAAAAGCAGGCT	Forward primer attaching US-GM-DS fragments to create the <i>pyrE</i> -GM fragment in second PCR step
GW-attB2	GGGGACCACTTTGTACAAGAAAGCTGGGT	Reverse primer attaching US-GM-DS fragments to create the <i>pyrE</i> -GM fragment in second PCR step

ChargeSwitch®-Pro Plasmid Miniprep kit (Carlsbad, CA, USA) according to the manufacturer's instructions. Analysis was done using *Xba*I restriction enzyme (NEB, MA, USA), which cuts at the flanking region of *aacC1*; resulted into three plasmid fragments which were analyzed with 1.5% agarose electrophoresis. The gateway plasmid containing the proper recombination was designated as pDONR-*pyrE*-GM. The pEX18ApGW plasmid was then mixed with pDONR-*pyrE*-GM and the Gateway® LR clonase enzyme (Invitrogen, CA, USA) at 50 ng/μl each following manufacturer's instructions. The plasmid was then transformed into *E. coli* (DH5α) and plated on LB agar plates containing 200 μg/ml ampicillin for selection of resistant colonies. A single resistant colony was then grown in LB broth with 200 μg/ml ampicillin and plasmid extraction was done.

2.1.3. Transformation and recombination

The constructed gateway plasmid was then transformed into *P. aeruginosa* by electroporation using a Gene Pulser Xcell™ Electroporation System (Bio-Rad Laboratories, CA, USA) utilizing the protocol adapted from Choi and Schweizer (2005). *P. aeruginosa* cells were incubated at 42 °C for 24 h; and centrifuged at 10,053 g for 2 min. The collected pellet was resuspended in 300 mM sucrose solution, wherein the cloned pEX18ApGW plasmid was added; and exposed to electroporation in a 2 mm gap electroporation cuvette. After 1 h incubation at 37 °C with shaking, the cell suspension was centrifuged; and the cell pellet was resuspended and plated on LB agar containing 30 μg/ml gentamicin. Resistant colonies were selected and grown on LB containing 5% sucrose to eliminate any merodiploids. Mutant *pyrE* was amplified and sent for sequencing at GENEWIZ Sequencing (South Plainfield, NJ, USA). The results were then run on NCBI Blast software for alignment results.

2.2. Analysis of growth curves

The growth curves of WT *P. aeruginosa* and Δ*pyrE* was measured according to the method described by Liu et al. (2020). Cells were grown until mid-log phase on OD600nm of 0.6 A in LB broth. A 500 μl of fresh inoculum was added to LB broth in a conical flask from the mid-log phase cells. For complementation with uracil, media containing 40 μg/ml uracil was added to the specific flask. Flasks were incubated at 37 °C with shaking at 220 rpm. Spectrophotometric readings of OD600nm were recorded hourly for 11 h on BioTek Synergy HT Microplate reader (Winooski, VA, USA).

2.3. Assessment of *P. aeruginosa* virulence and biofilm

2.3.1. Motility assays

Motility assays for twitching, swimming and swarming were studied. Twitching assay was done utilizing the procedure previously described (Rashid et al., 2000). Thin 3 mm layers of LB med-

ium solidified with 1.5% agar plates were prepared. For uracil-supplemented plates, 40 μg/ml uracil was added to the medium. A sterile needle was used to touch a fresh colony and stabbed into the agar to reach the sub-surface area. Plates were then incubated at 37 °C for 24 h. The twitching diameter was measured and plates were photographed using a Nikon D3100 DSLR camera.

Swimming assay was measured on plates containing 1% tryptone, 0.5% NaCl and 0.2% agar as previously described (Li et al., 2020). Using a sterile needle, a fresh colony was touched with the tip of the needle and stabbed halfway through the agar. Plates for complementation test were supplemented with 40 μg/ml uracil. All plates were incubated for 20 h at 30 °C. The diameter of the swimming zone was measured and the plates were imaged as mentioned previously.

Swarming assay was performed on semi-solid LB agar plates containing 0.5% agar and 5% glucose as previously described with slight modifications (Radulović et al., 2018). A fresh colony was transferred to 10 ml LB broth and grown for 24 h. Cells were then standardized to a final OD600nm of 0.6. A 1 ml broth was transferred to an Eppendorf tube and cells were centrifuged at 10,053 g for 2 min. Cells were resuspended in 50 μl fresh LB broth and 5 μl was transferred to the surface of the agar plate. Plates were incubated at 30 °C for 10 h; then left at room temperature for 20 h. Uracil-treated plates were supplemented with 40 μg/ml uracil. The zone of swarming was measured and the images of the plates were obtained.

2.3.2. Rhamnolipid production assay

Rhamnolipid production was measured using prepared LB plates supplemented with 0.2 g/L cetyltrimethylammonium bromide (CTAB) and 0.005 g/L methylene blue as previously described with slight modifications (Siegmond and Wagner, 1991). A hole was stabbed with a toothpick into the center of the agar surface and 5 μl of the cell supernatant in LB was added to the punched hole. The plates were left at room temperature for 5 days and the diameter of the observed halo represented the amount of rhamnolipid produced. The halo measurements were divided by the corresponding OD600nm readings to account for cell density.

2.3.3. Biofilm formation

Cells were grown to mid-log phase in to a final OD600nm of 0.6 A; and 1 μl of bacterial cells were added to fresh 100 μl LB in 96-well round bottom plates. The inoculated plates were incubated at 37 °C for 48 h; afterwards, the well content was aspirated, and washed thrice with sterile distilled water to remove unattached cells. The wells were subsequently dried and stained with 150 μl of 0.5% (w/v) crystal violet for 10 min. After repeated washing, the air-dried wells were filled with 200 μl of 100% ethanol. The plate was incubated at room temperature for 15 min and 490 nm readings were measured on BioTek Synergy HT Microplate reader

(Winooski, VA, USA) as previously described (O’toole and Kolter, 1998).

2.4. RT-qPCR analysis

Cells were grown in LB broth at 37 °C with shaking at 220 rpm for 24 h. A 1 ml inoculated broth was transferred to an Eppendorf tube and centrifuged at 10,053 g for 2 min. The collected cell pellet was used for total RNA extraction using HiGene™ Total RNA Prep Kit (BioFACT Co., Daejeon, South Korea) according to manufacturer’s instructions. RNA concentration and quality was determined using BioPhotometer Plus (Eppendorf, Germany). cDNA was synthesized using the FIREScript RT cDNA synthesis Kit (Solis BioDyne, Tartu, Estonia, <https://www.sbd.ee>) as per manufacturer’s instructions. Real-Time PCR was done on ABI 7500 Real-Time PCR System (Applied Biosystems, Darmstadt, Germany) using 5 × HOT FIREpol® EvaGreen® qPCR Supermix (Solis BioDyne, Tartu, Estonia, <https://www.sbd.ee>). 16S rRNA was used as the control. Genes selected in this study (Table 3) were determined to be associated with the motility of *P. aeruginosa*, as previously described (Hosseiniidoust et al., 2013). Relative microRNA expression profiles were determined and analyzed in Microsoft Excel spreadsheet.

2.5. Statistical analysis

All experiments were done in triplicate, and the data were presented as means ± standard deviations. Statistical comparison was done using Two-Way ANOVA followed by Tukey’s post-hoc test (GraphPad Prism software version 6.00 for Windows, La Jolla California, USA; <https://www.graphpad.com>). Results were statistically significant when a p-value ≤ 0.05 was obtained.

3. Results

3.1. Construction of the mutant

PCR amplification results revealed a fragment approximately 1700 bps in size resulting from the insertion of the *aacC1* gentamicin-resistant gene for the $\Delta pyrE$ and approximately 700 bps fragment resembling the wild type PA01 (Fig. 1A). Sequencing results revealed proper insertion of the *aacC1* and confirmed the deletion of the 74 bps fragment. Results for alignment of the DNA sequence on NCBI Blast software are demonstrated in Fig. 1B.

3.2. Growth curves

Growth curves for wild type and $\Delta pyrE$ revealed that there were no differences in growth on enriched media as both the bacterial

Table 3

List of genes and their target primer sequences used to study gene expression by RT-qPCR for both PA01, $\Delta pyrE$ and $\Delta pyrE+U$.

Gene	Primer sequence
<i>RhlA</i>	F- GGC GAT CGG CCA TCT G R- AGC GAA GCC ATG TGC TGA T
<i>PilA</i>	F- TGC GCG TTC GGA AGG T R- CGA CTC TTC AAC AGT GGT CTT CA
<i>PilI</i>	F- GCA CTG CAA CCC TTC ATT CAT R- CGC ATG CGG GCT GAA C
<i>RhlB</i>	F- GCC TGT CGG CGT TTC ATG R- CAT CCC CCT CCC TAT GAC AA
<i>FlhC</i>	F- CAG TGC CAA GGA CGA TGC T R- AAC GTT CAG ACC GCT GAT CTG
<i>FlhD</i>	F- TGG CTG GCA CCT ACC AGA TC R- GGC CTG GAG GGC AAT CTT
<i>AlgR</i>	F- CCT CGG CCA GCA ATG G R- CGG ATA TCC AGC AGG ACG AT

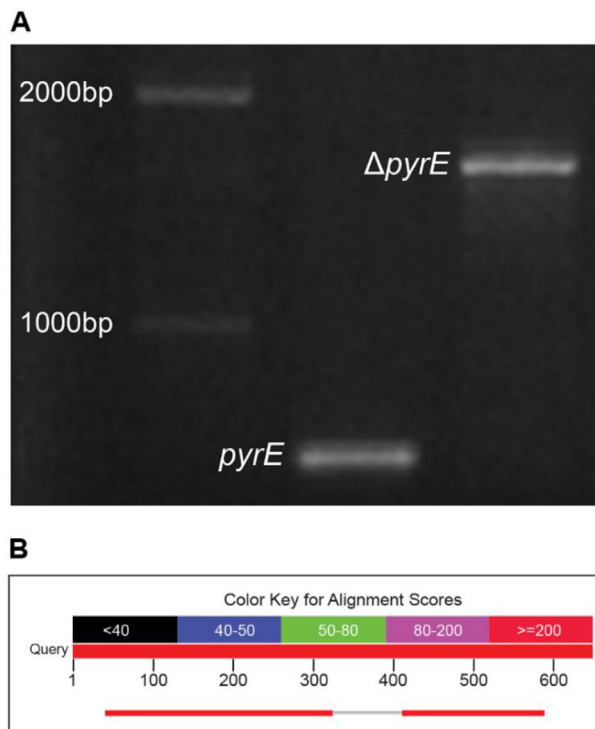


Fig. 1. (A) Agarose gel electrophoresis (1.5%) of wild type *pyrE* and $\Delta pyrE$ after PCR amplification. (B) Alignment results of $\Delta pyrE$ compared to WT *pyrE* demonstrating the deletion.

strains reached the stationary phase simultaneously. Whereas supplementation of the media with 40 µg/ml uracil did not have any considerable effect on the growth curves (Fig. 2).

3.3. Motility

All three types of motility observed were reduced as a result of the mutation (Fig. 3). Upon supplementation of uracil in the growth media of $\Delta pyrE$ ($\Delta pyrE+U$), the motility was restored to some extent but not comparable to the levels of the wild type strain. PA01 had mean diameters of 18 mm for twitching, 35 mm for swimming, and 12 mm for swarming. The $\Delta pyrE+U$ strain exhibited mean diameters of 10 mm for subsurface twitching, 15 mm for swimming and 8 mm for swarming. For the $\Delta pyrE$ strain, there was complete loss of twitching motility; and swimming and swarming motilities were severely diminished with the mean diameters being 3 mm and 4 mm respectively.

3.4. Rhamnolipid production

Rhamnolipid production was decreased in the $\Delta pyrE$ strain when compared to PA01 (Fig. 4A). The wild type exhibited a mean diameter of 16 mm for the rhamnolipid halo, while the $\Delta pyrE$ strain showed a 75% drop in production and had a mean diameter of only 6 mm for the rhamnolipid halo. On the contrary, $\Delta pyrE+U$ revealed a mean diameter of 10 mm for amount of rhamnolipid produced. Dividing the results by the OD600nm, the results were as follows, 13.3 for the wild type, 9.16 for $\Delta pyrE+U$ and 5 for the $\Delta pyrE$ strain (Fig. 4B).

3.5. Biofilm formation

Biofilm formation was reduced in the $\Delta pyrE$ strain when compared to PA01 by more than 50%. Supplementation with uracil

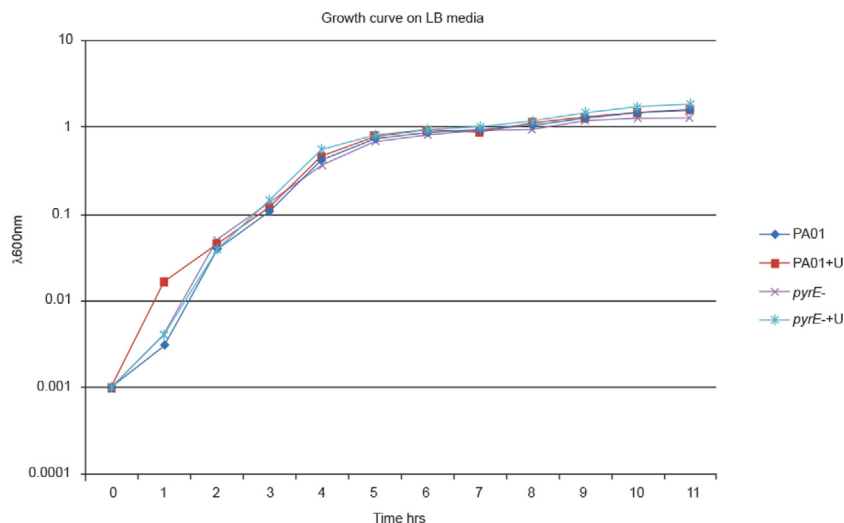


Fig. 2. Growth curves of wild type *P. aeruginosa* and mutant strains in LB with and without 40 μg/ml uracil supplementation.

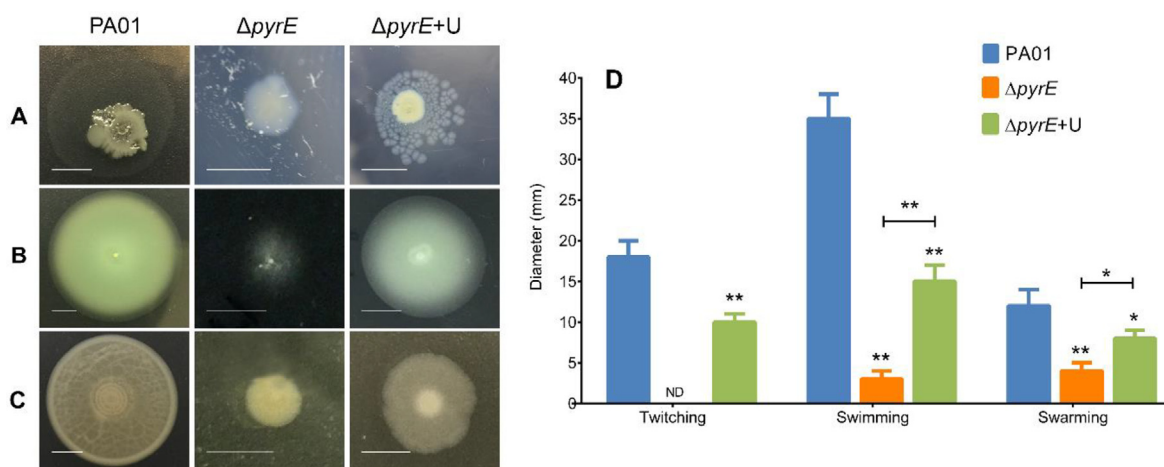


Fig. 3. Representative images of the effect of *pyrE* knockout on (A) twitching, (B) swimming and (C) swarming capabilities of *P. aeruginosa* PA01, $\Delta pyrE$ and $\Delta pyrE+U$ on LB agar plates. The intensive growth in the middle is the initial bacterial colony while the halo around the colony represents the twitching distance. (D) Mean twitching, swimming and swarming motilities of *P. aeruginosa* PA01, $\Delta pyrE$ and $\Delta pyrE+U$. Data are presented as means \pm SD, $n = 6$ (** $p \leq 0.01$ and * $p \leq 0.1$).

increased biofilm formation by about 30% but did not restore biofilm formation to the levels of the wild type strain (Fig. 5).

3.6. RT-qPCR

Real-time PCR results showed a statistically significant drop in gene expression for rhamnolipid, pili and flagella-producing genes, except for *fliD* and *algR* which are involved in biofilm formation, in the mutant when compared to the wild type. *fliD* showed a marked increase in expression when compared to the wild type and uracil-supplemented mutant strain. The $\Delta pyrE+U$ showed no change in the *fliD* expression after supplementation with uracil. It was also determined that after supplementation with uracil, the $\Delta pyrE+U$ showed even further decreased gene expression levels compared to $\Delta pyrE$; except for the *fliD* gene where there was no statistically significant change in gene expression (Fig. 6).

4. Discussion

The present study observed the inhibitory effect of the disruption of *de novo* pyrimidine synthesis pathway upon motility and

altered biofilm phenotype in *P. aeruginosa* (PA01) and $\Delta pyrE$ mutant. This was achieved through site-directed mutagenesis in the pyrimidine pathway, thereby leading to a complete halt in the pyrimidine biosynthesis in the mutant microorganism. Isaac and Holloway (1968) reported that the mutagenesis of the pyrimidine pathway lead to several mutant strains of *P. aeruginosa* and also studied their characteristics pertaining to decreased virulence. While modified biofilm production by different bacteria including *P. aeruginosa* through multiple genetic screens have been reported; construction of a site-directed mutagenesis is reportedly challenging (Hosseinioust et al., 2013; Morici et al., 2007). This study focused on site-directed mutagenesis as an essential element of protein engineering, wherein proteins suitable for structural characterization of the bacteria were selectively synthesized. The preference for studying *pyrE* mutation in *P. aeruginosa* PA01 were based on promising variations in the virulence of the mutant bacterium (Hosseinioust et al., 2013; Morici et al., 2007; Ralli et al., 2007). The mutation in this study by way of halting pyrimidine synthesis, forced the bacterium to salvage its pyrimidine from enriched media (Fig. 7). The net result was a decreased motility and biofilm formation as evidenced from the results, thereby rendering the bacterium less pathogenic.

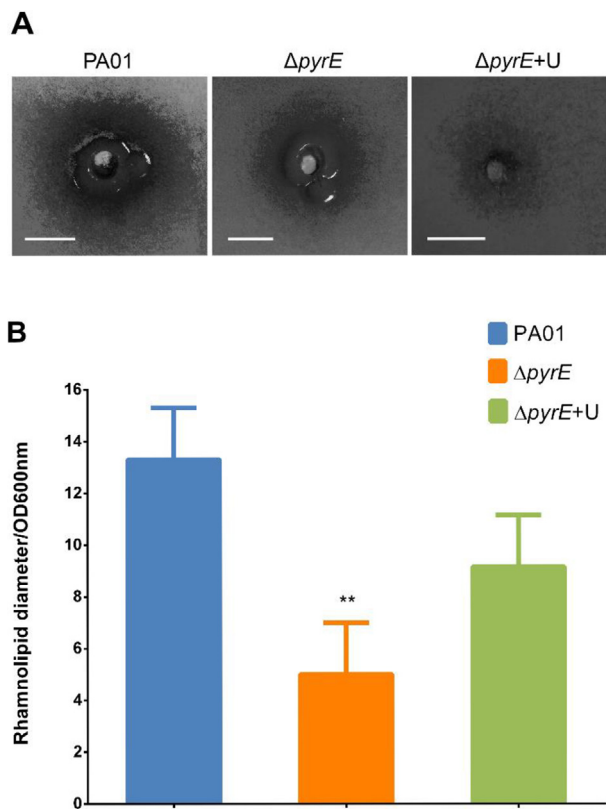


Fig. 4. (A) Representative images of the effect of *pyrE* knockout on rhamnolipid production for the halo produced by *P. aeruginosa* PA01 wild type, mutant and uracil-supplemented strains on mineral media. (B) Rhamnolipid production assay in wild type, $\Delta pyrE$ and the $\Delta pyrE+U$ strains after dividing OD600nm readings. Data are presented as means \pm SD, $n = 6$ (** $p \leq 0.01$).

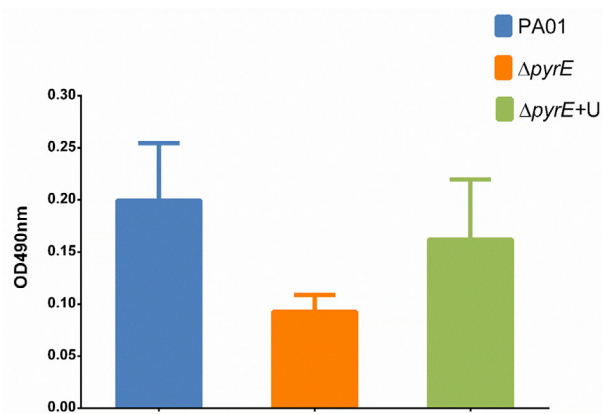


Fig. 5. Effect of *pyrE* knockout on biofilm production capabilities of the PA01, $\Delta pyrE$ and complemented $\Delta pyrE+U$ at crystal violet readings of OD490nm.

Based on the analysis of the growth curves in this study, it was found that enriched media had no effect on the patterns of growth in both the wild and mutant types of *P. aeruginosa*. However, upon supplementing the media with 40 $\mu\text{g/ml}$ uracil, the wild types had a shorter lag phase in comparison to an extended lag phase combined with faster log phase in the mutant bacteria, which were pyrimidine auxotrophs. Nevertheless, the mutant bacteria were unable to grow in minimal media without the addition of uracil (data not shown). The supplementation with uracil enabled the

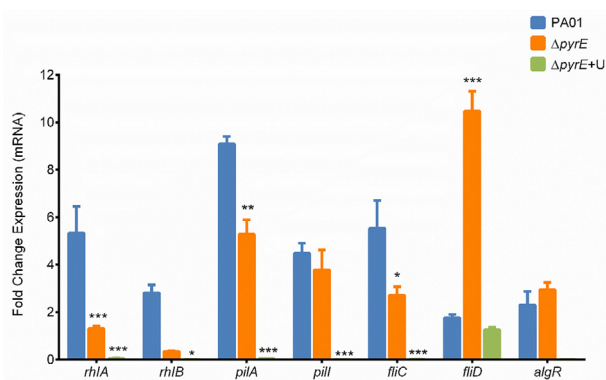


Fig. 6. Gene expression levels of selected genes involved in motility and biofilm formation of *P. aeruginosa* in wild type, mutant and uracil-supplemented strains. Data are presented as mean fold change \pm SD, $n = 6$ (** $p \leq 0.001$, ** $p \leq 0.01$, and * $p \leq 0.05$).

mutant bacteria to synthesize pyrimidines using the salvage pathway rather than the slower *de novo* pyrimidine pathway leading to hastened nucleotide synthesis and faster growth (Ralli et al., 2007). On the contrary, the PA01 exhibited slower growth owing to their functional *de novo* pyrimidine pathway.

One of the most important virulence factor of *P. aeruginosa* to cause life-threatening infections is its motility and ability to attach and colonize surfaces (Burrows, 2012; Hosseinioust et al., 2013; O'toole and Kolter, 1998). As a result, the mutant had marked reduction in swimming and swarming motilities, with a total loss of twitching, in comparison to PA01. However, all three forms of motility were restored in the mutant strain upon addition of uracil to the medium; indicating a correlation between motility and pyrimidine synthesis through the salvage pathway. Similarly, a decrease in rhamnolipid production and biofilm formation was also observed in the mutant bacteria in comparison to PA01. Nevertheless, uracil supplementation restored both rhamnolipid production and biofilm formation in the mutant strain to a considerable extent, which were not observed in the wild type PA01. The reduced motility of the $\Delta pyrE$ mutant, in spite of uracil supplementation, could be attributed to decreased rhamnolipid synthesis. More importantly, reduction in motility and biofilm formation in the mutant bacteria were a result of internal interference such as inhibition of quorum sensing, as there was no observable change in the growth capabilities of the wild type and mutant strains in enriched media (Bains et al., 2012; Morici et al., 2007; Ralli et al., 2007). This was further confirmed by qPCR findings of the present study which revealed a decrease in the genes expression of rhamnolipid, pili, and flagella markers in $\Delta pyrE$.

In this study, the growth rates of wild type and mutant strains were similar in enriched media, which were comparable to what was reported by Brichta (2003). Nevertheless, motility, rhamnolipid production, and biofilm formation were reduced in the mutant type when compared to the wild type PA01. Similar results were reported by Ralli et al. (2007), following a *pyrD* knockout mutation in *P. aeruginosa*. While reporting diminished motility, rhamnolipid production and biofilm formation, they also reported reduced expression of exoproducts such as casein protease, elastase, and hemolysins and decreased iron-binding capacity. They suggested a role in inducing mutagenesis in the pyrimidine pathway as a mechanism for eliminating *P. aeruginosa* infection in immunosuppressed individuals. The pyrimidine auxotrophy exhibited by the $\Delta pyrE$ mutant enhances its motility, rhamnolipid production and biofilm formation upon addition of uracil to the growth media. This is in accordance to earlier findings corroborat-

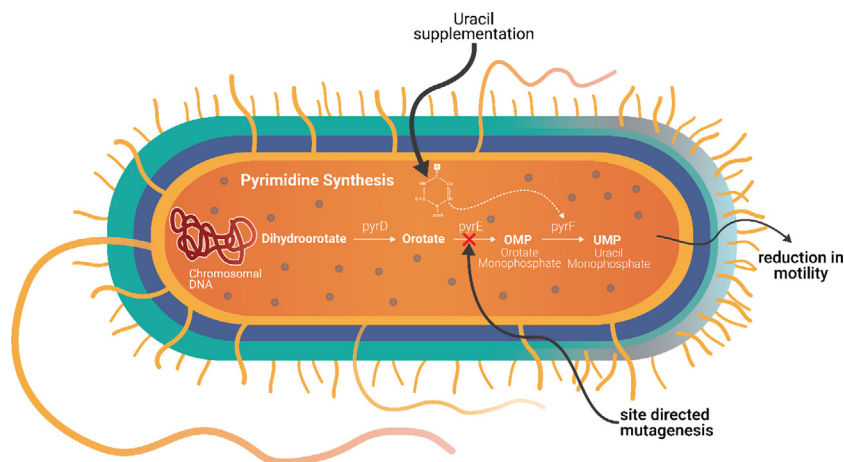


Fig. 7. Proposed mechanism of uracil complementation in *pyrE* mutation of *P. aeruginosa*.

ing pyrimidine auxotrophy with reduction in virulence factors of *P. aeruginosa* such as production of hemolysin, casein protease, elastase, pyoverdine, and pyocyanin (Ralli, 2005).

Although further gene expression studies regarding rhamnolipid, pili, and flagella function need to be further evaluated, the complementation of uracil in this study failed to restore normal gene expression in the mutant *pyrE* strain. Nonetheless, the decrease in the rhamnolipid gene expression observed in the present study has significant clinical implications, as rhamnolipids contribute to the ability of *P. aeruginosa* to resist antibacterial action of polymorphonuclear neutrophils (PMNs) in a biofilm environment (Donlan and Costerton, 2002). Based on these findings, there is potential use of DNA synthesis inhibitors specifically pyrimidine inhibitors as an alternative therapy to inhibit bacterial motility and biofilm formation in *P. aeruginosa* strains.

Fluorouracil (5-FU) is an anti-neoplastic drug that acts by blocking pyrimidine synthesis through inhibition of the enzyme thymidylate synthase (TS) (Attila et al., 2009). Fluorouracil has been known to cause antibacterial effects against oral microorganisms including *P. aeruginosa* at very high concentrations (>100 μM) (Vanlancker et al., 2016). Based on a study on *P. aeruginosa* PA14 strain by Ueda et al. (2009), 5-FU has the ability to suppress quorum sensing and biofilm formation through uracil-related mutations, namely *carA*, *carB*, *pyrB*, *pyrC*, *pyrD*, *pyrE*, and *pyrF*. Similar results were reported by Attila et al. (2009) with respect to the ability of 5-FU to inhibit biofilm formation and reduce virulence in *E. coli*. Using gold nanoparticle probes, Selvaraj and Alagar (2007) demonstrated the antibacterial capabilities of 5-FU against *P. aeruginosa*.

While bacteria efficiently develop resistance to inhibitors of bacterial growth such as antibiotics, the alternative approach of developing antibacterial drugs which inhibit virulence factors is gaining prominence (Attila et al., 2009; Guo et al., 2016). Guo et al. (2016) have reported the development of a novel compound against *P. aeruginosa*, with an ultimate aim of suppressing its virulence and antibiotic resistance. This novel treatment targets the *pyrD*, encoding for the PyrD protein. The PyrD protein is a dihydroorotate dehydrogenase (DHODase) involved in pyrimidine biosynthesis, similar to the PyrE protein investigated in the present study (Niazy and Hughes, 2015; Ralli et al., 2007). Donlan and Costerton (2002) also recommended a paradigm shift from the conventional strategies to eradicate biofilm-forming bacteria towards a futuristic approach based on inhibition of genes responsible for virulence factors such as cell adhesion, motility and rhamnolipid production.

5. Conclusions

The results of the present study revealed that *pyrE* mutants of *P. aeruginosa* PA01 exhibited a decrease in motility and biofilm formation capabilities as a result of the disruption of *de novo* pyrimidine synthesis. These findings demonstrate the importance of therapies targeting disruption of pyrimidine pathways, such as the *pyrE*, in order to treat recalcitrant *P. aeruginosa* infections similar to cystic fibrosis patients. Nevertheless, such possible therapies need to be validated further through molecular and clinical studies.

Conflict of interest

No conflict of interest declared.

Acknowledgements

The authors are grateful to Dr. Herbert Schweizer (Colorado State University, USA) for providing the gateway plasmids and Terrence Suministrado Sumague for assistance in preparing the figures and scientific illustrations. The authors would also like to thank Hadeel A. AlTulihe and Lorvijan G. Avila for their technical support.

Disclosure of funding

The authors extend their appreciation to the Deanship of Scientific Research at King Saud University for funding this work through research group No (RG-1439-026). The funders had no role in study design, data collection and analysis, decision to publish, or preparation of the manuscript.

References

- Attila, C., Ueda, A., Wood, T.K., 2009. 5-Fluorouracil reduces biofilm formation in *Escherichia coli* K-12 through global regulator AriR as an antivirulence compound. *Appl. Microbiol. Biotechnol.* 82, 525–533. <https://doi.org/10.1007/s00253-009-1860-8>.
- Bains, M., Fernández, L., Hancock, R.E.W., 2012. Phosphate starvation promotes swarming motility and cytotoxicity of *Pseudomonas aeruginosa*. *Appl. Environ. Microbiol.* 78, 6762–6768. <https://doi.org/10.1128/aem.01015-12>.
- Beckwith, J.R., Pardee, A.B., Austrian, R., Jacob, F., 1962. Coordination of the synthesis of the enzymes in the pyrimidine pathway of *E. coli*. *J. Mol. Biol.* 5, 618–634. [https://doi.org/10.1016/s0022-2836\(62\)80090-4](https://doi.org/10.1016/s0022-2836(62)80090-4).
- Behzadi, P., Baráth, Z., Gajdács, M., 2021. It's not easy being green: a narrative review on the microbiology, virulence and therapeutic prospects of multidrug-resistant *Pseudomonas aeruginosa*. *Antibiotics* (Basel, Switzerland). 10, 42. <https://doi.org/10.3390/antibiotics10010042>.

- Brichta, D.M., 2003. Construction of a *Pseudomonas aeruginosa* Dihydroorotase Mutant and the Discovery of a Novel Link Between Pyrimidine Biosynthetic Intermediates and the Ability to Produce Virulence Factors. University of North Texas.
- Brichta, D.M., Azad, K.N., Ralli, P., O'Donovan, G.A., 2004. *Pseudomonas aeruginosa* dihydroorotases: a tale of three pyrCs. *Arch. Microbiol.* 182 (1), 7–17.
- Burrows, L.L., 2012. *Pseudomonas aeruginosa* twitching motility: Type IV Pili in action. *Annu. Rev. Microbiol.* 66, 493–520. <https://doi.org/10.1146/annurev-micro-092611-150055>.
- Chadha, J., Harjai, K., Chhibber, S., 2021. Revisiting the virulence hallmarks of *Pseudomonas aeruginosa*: a chronicle through the perspective of quorum sensing. *Environ. Microbiol.* <https://doi.org/10.1111/1462-2920.15784>.
- Choi, K.-H., Schweizer, H. P., 2005. An improved method for rapid generation of unmarked *Pseudomonas aeruginosa* deletion mutants. *BMC Microbiol.* 5, 30–30. <https://doi.org/10.1186/1471-2180-5-30>.
- Donlan, R.M., Costerton, J.W., 2002. Biofilms: survival mechanisms of clinically relevant microorganisms. *Clin. Microbiol. Rev.* 15, 167–193. <https://doi.org/10.1128/cmr.15.2.167-193.2002>.
- Garavaglia, M., Rossi, E., Landini, P., Marinus, M.G., 2012. The pyrimidine nucleotide biosynthetic pathway modulates production of biofilm determinants in *Escherichia coli*. *PLoS ONE* 7 (2).
- Guo, Q., Wei, Y., Xia, B., Jin, Y., Liu, C., Pan, X., Shi, J., Zhu, F., Li, J., Qian, L., Liu, X., Cheng, Z., Jin, S., Lin, J., Wu, W., 2016. Identification of a small molecule that simultaneously suppresses virulence and antibiotic resistance of *Pseudomonas aeruginosa*. *Sci. Rep.* 6, 19141. <https://doi.org/10.1038/srep19141>.
- Horcajada, J.P., Montero, M., Oliver, A., Sorlí, L., Luque, S., Gómez-Zorrilla, S., Benito, N., Grau, S., 2019. Epidemiology and treatment of multidrug-resistant and extensively drug-resistant *Pseudomonas aeruginosa* infections. *Clin. Microbiol. Rev.* 32, e00031–e119. <https://doi.org/10.1128/cmr.00031-19>.
- Hosseindoust, Z., Tufenkji, N., Van De Ven, T.G.M., 2013. Predation in homogeneous and heterogeneous phage environments affects virulence determinants of *Pseudomonas aeruginosa*. *Appl. Environ. Microbiol.* 79, 2862–2871. <https://doi.org/10.1128/aem.03817-12>.
- Isaac, J.H., Holloway, B.W., 1968. Control of pyrimidine biosynthesis in *Pseudomonas aeruginosa*. *J. Bacteriol.* 96, 1732–1741. <https://doi.org/10.1128/jb.96.5.1732-1741.1968>.
- Jurado-Martín, I., Sainz-Mejías, M., McClean, S., 2021. *Pseudomonas aeruginosa*: an audacious pathogen with an adaptable arsenal of virulence factors. *Int. J. Mol. Sci.* 22, 3128. <https://doi.org/10.3390/ijms22063128>.
- Kazmierczak, B.I., Schniederberend, M., Jain, R., 2015. Cross-regulation of *Pseudomonas* motility systems: the intimate relationship between flagella, pili and virulence. *Curr. Opin. Microbiol.* 28, 78–82. <https://doi.org/10.1016/j.mib.2015.07.017>.
- Kühn, M.J., Talà, L., Inclan, Y.F., Patino, R., Pierrat, X., Vos, I., Al-Mayyah, Z., Macmillan, H., Negrete Jr., J., Engel, J.N., Persat, A., 2021. Mechanotaxis directs *Pseudomonas aeruginosa* twitching motility. *PNAS* 118. <https://doi.org/10.1073/pnas.2101759118>.
- Li, Y., Xia, H., Bai, F., Song, X., Zhuang, L., Xu, H., Zhang, X., Zhang, X., Qiao, M., 2020. PA5001 gene involves in swimming motility and biofilm formation in *Pseudomonas aeruginosa*. *Microb. Pathog.* 144. <https://doi.org/10.1016/j.micpath.2020.103982>.
- Liu, X., Cai, J., Chen, H., Zhong, Q., Hou, Y., Chen, W., Chen, W., 2020. Antibacterial activity and mechanism of linalool against *Pseudomonas aeruginosa*. *Microb. Pathog.* 141.
- Malhotra, S., Hayes Jr., D., Wozniak, D.J., 2019. Cystic Fibrosis and *Pseudomonas aeruginosa*: the Host-Microbe Interface. *Clin. Microbiol. Rev.* 32, e00138–e218. <https://doi.org/10.1128/cmr.00138-18>.
- Morici, L.A., Carterson, A.J., Wagner, V.E., Frisk, A., Schurr, J.R., zu Bentrup, K.H., Hassett, D.J., Iglewski, B.H., Sauer, K., Schurr, M.J., 2007. *Pseudomonas aeruginosa* AlgR represses the Rhl quorum-sensing system in a biofilm-specific manner. *J. Bacteriol.* 189 (21), 7752–7764.
- Niazy, A., Hughes, L.E., 2015. Accumulation of pyrimidine intermediate orotate decreases virulence factor production in *Pseudomonas aeruginosa*. *Curr. Microbiol.* 71, 229–234. <https://doi.org/10.1007/s00284-015-0826-6>.
- Niazy, A.A., 2021. LuxS quorum sensing system and biofilm formation of oral microflora: a short review article. *Saudi Dental J.* 33, 116–123. <https://doi.org/10.1016/j.sdentj.2020.12.007>.
- O'Donovan, G.A., Neuhaard, J., 1970. Pyrimidine metabolism in microorganisms. *Bacteriol. Rev.* 34 (3), 278–343.
- O'toole, G.A., Kolter, R., 1998. Flagellar and twitching motility are necessary for *Pseudomonas aeruginosa* biofilm development. *Mol. Microbiol.* 30, 295–304. <https://doi.org/10.1046/j.1365-2958.1998.01062.x>.
- Parkins, M.D., Somayaji, R., Waters, V.J., 2018. Epidemiology, biology, and impact of clonal *Pseudomonas aeruginosa* infections in cystic fibrosis. *Clin. Microbiol. Rev.* 31, e00019–e118. <https://doi.org/10.1128/cmr.00019-18>.
- Radulović, N.S., Stojanović, N.M., Glišić, B.Đ., Randjelović, P.J., Stojanović-Radić, Z.Z., Mitić, K.V., Nikolić, M.G., Djuran, M.I., 2018. Water-soluble gold(III) complexes with N-donor ligands as potential immunomodulatory and antibiofilm agents. *Polyhedron* 141, 164–180. <https://doi.org/10.1016/j.poly.2017.11.044>.
- Ralli, P., Srivastava, A.C., O'donovan, G., 2007. Regulation of the pyrimidine biosynthetic pathway in *apyrD* knockout mutant of *Pseudomonas aeruginosa*. *J. Basic Microbiol.* 47, 165–173. <https://doi.org/10.1002/jobm.200610248>.
- Ralli, P., 2005. Impaired Virulence factor Production in a Dihydroorotate Dehydrogenase Mutant (*pyrD*) of *Pseudomonas aeruginosa*. University of North Texas.
- Rashid, M.H., Rao, N.N., Kornberg, A., 2000. Inorganic polyphosphate is required for motility of bacterial pathogens. *J. Bacteriol.* 182, 225–227. <https://doi.org/10.1128/jb.182.1.225-227.2000>.
- Redfern, J., Wallace, J., van Belkum, A., Jaillard, M., Whittard, E., Ragupathy, R., Verran, J., Kelly, P., Enright, M.C., 2021. Biofilm associated genotypes of multiple antibiotic resistant *Pseudomonas aeruginosa*. *BMC Genomics* 22 (1), 1–16.
- Selvaraj, V., Alagar, M., 2007. Analytical detection and biological assay of antileukemic drug 5-fluorouracil using gold nanoparticles as probe. *Int. J. Pharm.* 337, 275–281. <https://doi.org/10.1016/j.ijpharm.2006.12.027>.
- Siegmund, I., Wagner, F., 1991. New method for detecting rhamnolipids excreted by *Pseudomonas* species during growth on mineral agar. *Biotechnol. Tech.* 5, 265–268. <https://doi.org/10.1007/bf02438660>.
- Srinivasan, R., Santhakumari, S., Poonguzhali, P., Geetha, M., Dyavaiah, M., Xiangmin, L., 2021. Bacterial biofilm inhibition: a focused review on recent therapeutic strategies for combating the biofilm mediated infections. *Front. Microbiol.* 12, 676458. <https://doi.org/10.3389/fmicb.2021.676458>.
- Talà, L., Fineberg, A., Kukura, P., Persat, A., 2019. *Pseudomonas aeruginosa* orchestrates twitching motility by sequential control of type IV pili movements. *Nat. Microbiol.* 4, 774–780. <https://doi.org/10.1038/s41564-019-0378-9>.
- Ueda, A., Attila, C., Whiteley, M., Wood, T.K., 2009. Uracil influences quorum sensing and biofilm formation in *Pseudomonas aeruginosa* and fluorouracil is an antagonist. *Microb. Biotechnol.* 2, 62–74. <https://doi.org/10.1111/j.1751-7915.2008.00060.x>.
- Vanlancker, E., Vanhoecke, B., Smet, R., Props, R., Van De Wiele, T., 2016. 5-Fluorouracil sensitivity varies among oral micro-organisms. *J. Med. Microbiol.* 65, 775–783. <https://doi.org/10.1099/jmm.0.000292>.
- Winkler, J.K., Suttle, D.P., 1988. Analysis of UMP synthase gene and mRNA structure in hereditary orotic aciduria fibroblasts. *Am. J. Hum. Genet.* 43, 86.
- Womack, J.E., O'donovan, G.A., 1978. Orotic acid excretion in some wild-type strains of *Escherichia coli* K-12. *J. Bacteriol.* 136, 825–827. <https://doi.org/10.1128/jb.136.2.825-827.1978>.
- Zifodya, J.S., Crothers, K., 2019. Treating bacterial pneumonia in people living with HIV. *Expert Rev. Respir. Med.* 13 (8), 771–786.